



Guide Column Array: A Versatile Approach to Aligning and Patterning Ceramic Nanofibers

Journal:	<i>Nanoscale</i>
Manuscript ID	NR-ART-07-2018-005635.R2
Article Type:	Paper
Date Submitted by the Author:	23-Oct-2018
Complete List of Authors:	Budi, Maeve; University of Florida, Materials Science & Engineering Kubart, Austin; University of Florida, Materials Science & Engineering Andrew, Jennifer; University of Florida, Materials Science & Engineering



Guide Column Array: A Versatile Approach to Aligning and Patterning Ceramic Nanofibers

Received 00th January 20xx,
Accepted 00th January 20xx

Maeve A. K. Budi[†], Austin Kubart[†] and Jennifer S. Andrew^{* a}

DOI: 10.1039/x0xx00000x

www.rsc.org/

Ceramic fibers have been manufactured via electrospinning for a variety of applications, including microelectronics, gas sensing, as well as in memory systems. Preferentially ordering ceramic fibers as uniaxially aligned mats, as layered arrays, or as patterned structures holds enormous potential to enhance current applications and add utility to electrospun ceramic fibers. Here, we developed a versatile guide column array-based method for manufacturing uniaxially aligned and patterned arrays of ceramic fibers. The guide column array was designed to control the electrospinning jet via electrostatic interactions between the electrified jet and the electrodes, resulting in fibers that preferentially oriented during deposition. A relationship between the ceramic precursor solution conductivity was correlated to the optimal operating voltage for the realization of aligned ceramic nanofibers using the guide column array.

1. Introduction

Electrospinning is a versatile technique used to manufacture fibers for a variety of applications including gas sensing, tissue engineering, superhydrophobic surfaces, and microelectronics^{1–6}. Each specific application may require a different morphology of the nanofibers. For example, specific applications may require fibers to be manufactured such that the fiber arrays are randomly orientated, are in uniaxially aligned layers, or form in a patterned array. While electrospinning has predominantly been used to fabricate polymer nanofibers, electrospinning methods have been applied to ceramic sol-gel systems to manufacture tailorable ceramic fibers to enhance the utility and properties of the ceramic. However, compared to polymers ceramic systems introduce additional variables that can complicate the electrospinning process, such as increased solution conductivity as well as considering the sol-gel hydrolysis and condensation reactions that are taking place. These differences between the properties of sol-gel ceramic systems and polymer systems, in addition to the the high variability of properties between different ceramic systems present challenges in fabricating uniaxially aligned ceramic systems. However, the ability to fabricate high surface area ceramic

nanofibers with tailorable morphologies would be highly appealing for device manufacturing⁷. The overall utility and performance of fibers can be enhanced based on the fiber collection methods used in the electrospinning phase of productions⁸.

A wide variety of ceramic fibers have been synthesized via electrospinning, where the vast majority of ceramic fibers manufactured via electrospinning consist of randomly oriented mats^{9–15}. However, compared to the polymer literature there are limited reports of ceramic nanofibers that have been electrospun in aligned or patterned arrays¹⁶. While several techniques to align fibers in polymer systems have been reported, considerably fewer have been presented for ceramic systems. Additionally, when compared to polymers for aligning ceramic nanofibers there is the the additional consideration that alignment must be maintained during calcination¹⁷. An easily transferable method that aligns ceramic fibers during the electrospinning process would be useful for creating ceramic fibers for a range of electronic applications. In this paper, we present a technique that can produce uniaxially aligned arrays of ceramic fibers that can be readily transferred to a wide range of systems without intensive optimization.

1.1 Aligned Electrospinning

^a 100 Rhines Hall, Dept. of Materials Science & Engineering, University of Florida, Gainesville, FL 32611-6400

[†] Equal contributions

Electronic Supplementary Information (ESI) available: [details of any supplementary information available should be included here]. See DOI: 10.1039/x0xx00000x

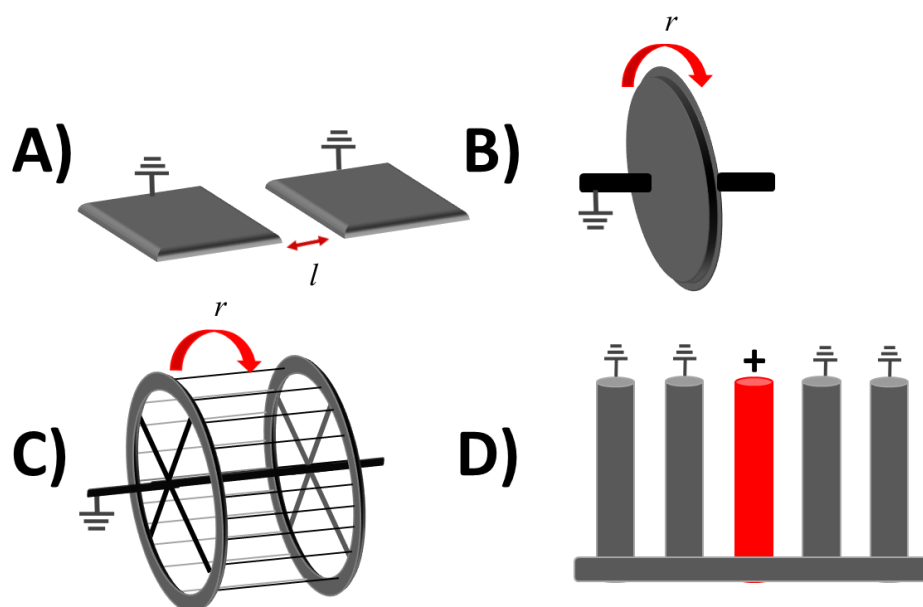


Figure 1. Alignment collector morphologies. A) Split electrodes separated by an insulating air gap; B) Spinning disc with a narrow edge; C) Rotating mandrel; and D) Proposed guide array collector.

To develop methods to align electrospun nanofibers, it is first necessary to take a look at the underlying principles that drive electrospinning. In a typical electrospinning process, a droplet is extruded from a metal syringe tip that is connected to a positive high voltage power supply. When a positive potential is applied the droplet at the syringe tip becomes electrified and is distorted into a conical shape, known as the Taylor cone. The Taylor cone forms due to electrostatic repulsion between surface charges and the Coulombic force exerted by the external electric field between the syringe tip and the collector. When a sufficiently high voltage is applied the electrostatic repulsion between charges accumulating on the surface of the droplet overcome the surface tension of the solution and a charged viscoelastic jet is ejected from the syringe tip towards a collector plate¹⁸. As the jet transports to the collector, solvent is evaporated, and a combination of viscoelastic restoring forces and Coulombic repulsion act to elongate the electrified jet, often also resulting in the formation of a growing bending instability¹⁹. The orders of bending instabilities create a whipping motion responsible for creating a random entanglement of fibers when collected on a grounded plate⁷. For polymer systems, the physical solution properties, such as conductivity and viscosity, are well described and don't vary significantly. However, for ceramic systems, these parameters, such as conductivity, can span several orders of magnitudes, from $\mu\text{S}/\text{cm}$ to mS/cm . This wide range of conductivity makes it very challenging to optimize an electrospinning technique for ceramic fiber alignment that can be transferable across multiple ceramic systems.

Fiber alignment methods used during electrospinning are shown in **Figure 1** and focus on two main mechanisms that dominate the jet behavior: Coulombic interactions (Figure 1a) with the collector and/or the mechanical movement of the jet (Figure 1b-c)^{11,17}. In polymer systems, alignment can be achieved by replacing the collector with two isolated plates that are separated by an insulating gap as seen in **Figure 1a**. As

a discrete fiber is deposited on a plate, it leaves a momentary charge on the contacted plate which exerts some finite electrostatic force on the trailing jet. This causes the trailing jet to deflect to the neighboring plate^{11,20}. The deposited fiber then spans the gap perpendicular to the plates. Fibers that are already deposited retain their charge in areas that are not in the relative vicinity of the grounded contacts, due to the low conductivity of polymers. Subsequent fibers will have the same charge as the initially deposited fiber, and will thus repel one another, resulting in aligning incoming fibers with the already deposited fibers²⁰.

With time, the fibers spanning the insulated gap begin to lose their charge by either interaction with the insulating material in the gap between the plates or via conduction to the grounded plate. The fibers then begin to behave as a homogenous grounded plate, where subsequent fibers are collected in a random alignment. This method has been improved by substituting highly insulating materials or high dielectric constant materials for the air gap. These properties preserve charges within the fibers to allow for longer deposition times and thicker mats before alignment is lost²⁰. Therefore, as this method is transferred to systems with higher conductivities, the ability to align using this technique is limited due to the higher rate of charge loss on the deposited fibers of more conductive systems²¹.

Mechanical methods have also been used to align polymer systems. In this case, fibers are electrospun onto a rotating mandrel; as the mandrel rotates, the mandrel draws out the fiber, creating a tensile force that acts to align the fiber as seen in **Figure 1b**^{17,22}. For this to be implemented successfully, several parameters need to be optimized for both polymer and ceramic systems. These parameters include mandrel rotation rate, solution viscosity, the distance between the syringe tip and the collector, syringe pump rate, humidity, applied voltage, and mandrel dimensions¹⁷.

For polymer systems, many of these parameters are fairly consistent from one polymer system to another, making this

method easily transferable. On the other hand, in ceramic systems there can be a large variability in properties across systems, so transferring operating parameters between ceramic systems is not a viable option. In particular, the higher conductivities of ceramic precursor solutions leads to increased instabilities in the electrified jet, making it more challenging to align solely via mechanical approaches. Additional alignment systems exist that contain variations and combinations of the core concepts outlined in the Coloubic and mechanical methods, an example of which is shown in **Figure 1c**^{23,24}. Although many advanced systems exist for the alignment of polymer systems, a consistent, easily optimized system that can handle a wide variety of ceramic systems is lacking. This paper develops a simple guide column-based method to align ceramic fibers during electrospinning solely by leveraging electrostatic interactions. This guide column method uses an array of five conductive columns that are separated by an air gap as displayed in **Figure 1d**. The central guide column is positively charged via a DC power supply while the adjacent columns are grounded. A conductive ring is placed around the needle tip and charged using the same power supply that is connected to the needle to focus the jet on the guide column^{25–28}. This focusing ring seeks to create a more homogenous field at the needle tip, which also promotes fiber deposition towards the grounded collector. As the electrified jet approaches the guide column, the repulsive Coulombic forces deflect the fiber to the nearest grounded column, where the approaching fiber is able to dissipate charge. The deposited fiber is then attracted back to the central guide column via the same Coulombic forces that repelled it initially.

Due to the constant electric field between columns, the fibers maintain a degree of polarization that aids in repelling and aligning the nearby fibers. Therefore, as more fibers are deposited, the degree of alignment will increase. This method is capable of fabricating thick fiber mats of highly aligned ceramic fibers. Since the mechanics of this method primarily act on the response of the fibers to the electrostatic forces of the column array, once the conductivity of the precursor solution is known the optimal alignment conditions can be identified. Specifically, the conductivity of the precursor solution has been correlated to the required voltage applied to the guide column to achieve the highest degree of alignment. Thus, this method can easily align large quantities of ceramic fibers by utilizing the relationship between ceramic precursor solution conductivity and guide column voltage.

Here, we demonstrate the versatility of this guide column array through the successful alignment of a range of functional ceramic materials. Furthermore, a relationship between the optimum guide column voltage and the conductivity of the electrospinning solution was established. With this relationship, new ceramic electrospinning solutions could be aligned if their conductivity is known.

1.2 Patterned Electrospinning

Continuing off principles used to design and test the guide column array; a grid collector was designed to pattern aligned fiber systems orthogonal to one another. This substrate is shown in **Figure 2**, where four copper plates are paired directly opposite to one another across a circle 2 cm in diameter. Using this substrate aligned fibers can be formed when voltage is applied to one contact while grounding the opposite

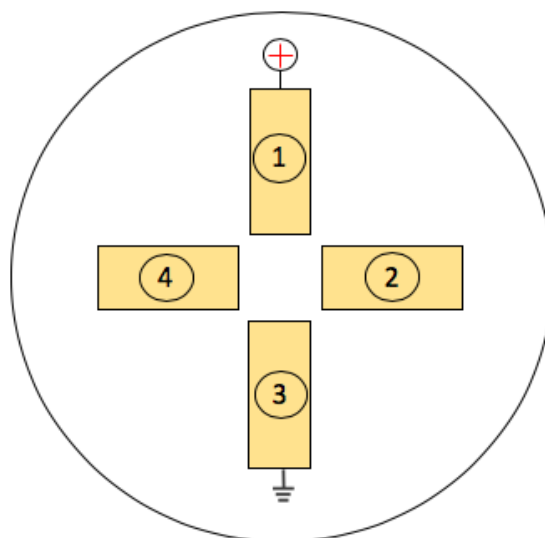


Figure 2: 2D schematic of grid collector featuring the four copper plates used to pattern aligned fiber layers orthogonal to one another. To form the first layer, electrodes 1 and 3 were attached to a positive voltage supply and grounded, respectively. To form the orthogonal layer the power supply was then connected to electrode 2 while 4 was grounded.

contact. Alternating the pair of contacts that creates an electric field manufactures aligned layers orthogonal to one another.

2. Methods

2.1 Set-up and Electrospinning

2.1.1 Guided Array Set-Up and Electrospinning

The guided array, shown in Figure 1d, was created by spacing five 20 cm long, 0.5 cm diameter, copper tubing columns 2 cm apart. A high voltage power supply was connected to the center column while the remaining columns were grounded. Solutions from previously established electrospinning systems were chosen from literature; specifically, BaTiO₃, CoFe₂O₄, Ni_{0.5}Zn_{0.5}Fe₂O₄, and BiFeO₃ were prepared^{9,10,12–15}. As an example, the CoFe₂O₄ solution was prepared by mixing stoichiometric amounts of ferric nitrate and cobalt acetate in 2 mL of acetic acid and 1.5 mL of 2-methoxy ethanol. At the same time a polymer solution was prepared where 0.5 g of polyvinylpyrrolidone (PVP) was dissolved in 1.75 mL of ethanol and 1.45 mL of dimethyl formamide. Once both solutions were dissolved the ceramic precursor solution was slowly added to the polymer solution. The resultant mixture was then stirred for 12h. The prepared solutions were loaded into a 3 mL syringe and the syringe was loaded into a syringe pump located within an electrospinning chamber. The syringe pump was positioned so that the needle tip pointed directly towards the central column of the array at a distance of 28 cm. A 6 cm diameter conductive loop was electrically contacted to the needle and suspended roughly 1 cm behind the tip so that it is perpendicular to the length of the needle. A high voltage power supply was attached to the needle and conductive loop. Relative humidity was lowered inside the chamber to between 30% and 40% relative humidity. Voltage values ranging from 1-10 kV were applied to the central column of the guide array.

The solution flow rate and applied syringe tip voltage were determined from previously reported methods and remained constant within each fiber system.

2.1.2 Grid Array Set-Up and Electrospinning

A grid array was constructed by setting four 1 cm x 3 cm x 0.3 cm copper plates into a cross formation as shown in Figure 2. The plates were fixed and set into epoxy. Once cured, the surface was polished to reveal the copper plates. Insulated 18 AWG copper wiring was connected to the plates prior to being set in epoxy. A high voltage power supply was connected to one plate while the plate opposite was grounded. The remaining plates are left unconnected. After electrospinning for five minutes, deposition was paused. The high voltage power supply was then moved from the current plate to the adjacent one and the grounded connection is moved to the plate opposite to the newly charged plate so that the new electric field will be orthogonal to the previous one. Electrospinning was then resumed, creating a subsequent layer of fibers that was aligned perpendicular to the previous

needle. Relative humidity was lowered inside the chamber to between 30% and 40% relative humidity and was maintained throughout the electrospinning process at room temperature. Voltage values ranging from 1-6 kV were applied to the plates. The solution extrusion rate and applied needle voltage were determined from previously reported methods and remained constant within each fiber system¹².

2.2 Calcination

Continuous mats of aligned fibers were removed from the guide column array. The layered mats of fibers were then dried in a vacuum oven at 75°C for 24 hours to ensure full solvent evaporation. The fibers were then placed in a furnace and heated to 250°C at a ramp rate of 2°C/minute and held for one hour to burn off the polymer. The temperature was then increased at 2°C/min to the final temperature required to develop the ceramic phase. The final temperature and dwell time required to develop the ceramic phase were determined by previously reported conditions. For example, the CoFe₂O₄ fibers were heated to 600°C and held for 3 hours.

2.3 Characterization

Fiber mats were characterized using scanning electron microscopy (SEM) with the FEI Nova 430 and the Phenom ProX desktop SEM. The fiber mats were imaged both "as-spun" and post-calcination. ImageJ analysis software was used to measure the alignment of the fibers by measuring angle of the

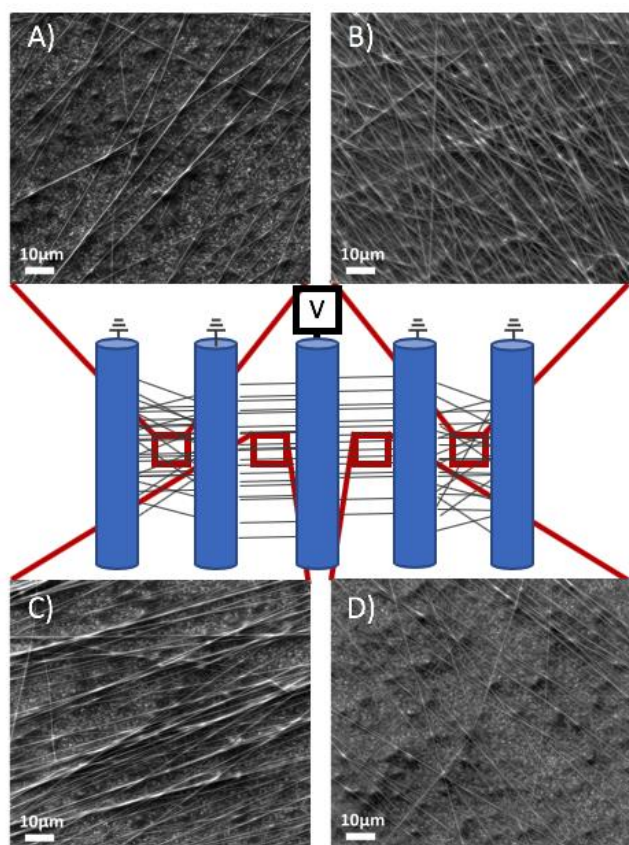


Figure 3. CoFe₂O₄ fiber alignment at different collection points with the guided column array with a guide column voltage of 6kV. Respectively, the outermost gaps show mainly randomly orientated fibers.

layer.

For the grid array, BaTiO₃ and CoFe₂O₄ solutions used in the previous section were once again prepared^{12,14,15}. As above, the prepared solutions were loaded into a 3 mL syringe and the syringe was loaded into a syringe pump located within the electrospinning chamber at a distance of 16 cm from the collector. A high voltage power supply was connected to the

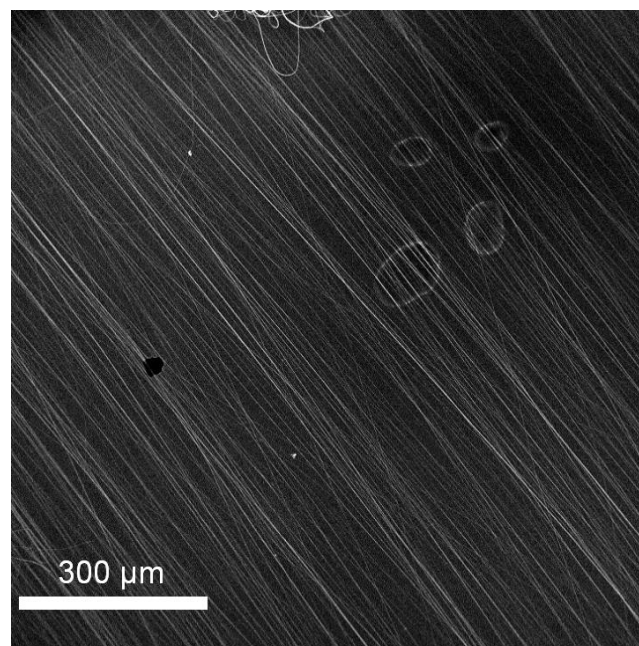


Figure 4. SEM image of highly aligned as-electrospun CoFe₂O₄ fibers electrospun using the guide column array.

fibers with respect to a constant axis. The distribution of fiber angles was plotted in a histogram, and alignment was defined as fibers within a 25° distribution orthogonal to the guide column.

Conductivities of the precursor solutions were measured with an Accumet Excel XL20 conductivity probe. The crystalline phases of calcined nanofiber arrays were characterized with X-

ray diffraction using a Panalytical X'PERT powder diffractometer with a copper anode tube.

3. Results and Discussion

3.1 Insulating Gap versus Guide Column Array

To verify the utility of the guide column array on fiber alignment, both CoFe_2O_4 and BaTiO_3 fibers were spun with a central guide column voltage ranging from 1-6kV. Fiber deposition between the center guide column and the adjacent columns was altered with the addition of the applied voltage to the central column. This was expected, as the voltage applied to the central column distorts the electrostatic field the electrospinning jet experiences as it approaches the collector. There was some build-up of randomly aligned fibers on the edges of the central columns (columns 2 and 4), however the addition of the two additional flanking columns, the random build-up is directed to deposit between the grounded columns and does not interfere with the aligned mat in the center. This is demonstrated in Figure 3, which show CoFe_2O_4 fibers that were electrospun using a guide column voltage of 6 kV. Each sample exhibited some degree of alignment (Figure S1), however, the samples from the interior, specifically the columns immediately flanking the guide column, have a greater degree of alignment than samples further from the guide column. This was expected, as the electrostatic interactions between the fiber jet and the guide

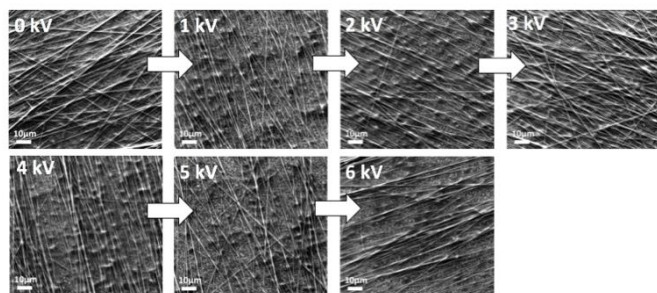


Figure 5. SEM samples showing an increase in alignment with increasing central guide column voltage for CoFe_2O_4 . Guide column voltages are listed on each SEM image. Alignment increases until a maximum alignment is reached at a central guide column voltage of 6 kV.

column are what drives the alignment, it follows that the alignment will no longer be as prominent as the fibers travel further from the guide column. Subsequent samples were all taken from the regions immediately flanking the guide column.

These results highlight the critical role electrostatic interactions play in the alignment of ceramic nanofibers, and that the presence of an insulating gap alone is insufficient. Samples taken from the outer gap between the outermost two grounded electrodes are randomly orientated (Figure 3); thus, the presence of an insulating gap is not sufficient to stimulate high degrees of alignment in conductive ceramic sol-gel based fibers. Additionally, when the outermost grounded columns were removed the overall yield of aligned fibers between the central column and the adjacent grounded column decreased. On the other hand, the samples taken directly between the

central column and the adjacent grounded columns where there is a constant electric field exhibit a high degree of alignment. Several trials with CoFe_2O_4 fibers were completed to ensure the repeatability of this approach and Figure 4 shows highly aligned fibers.

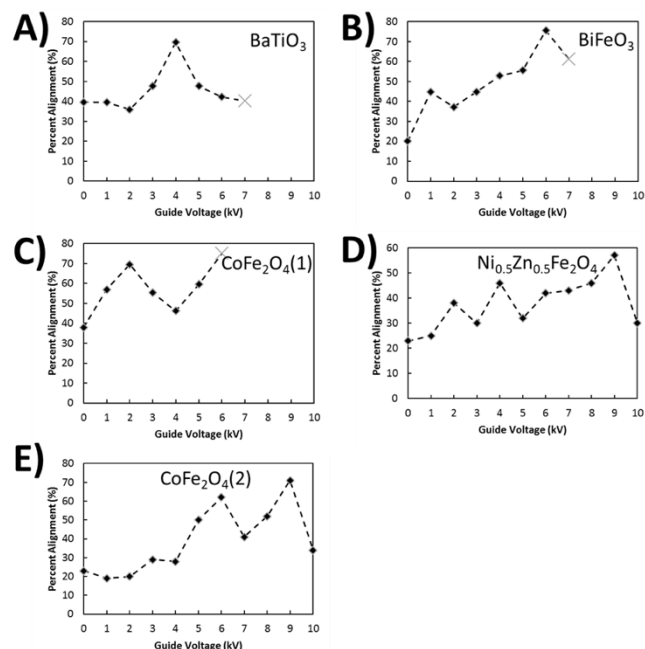


Figure 6. Plots of each fiber system showing the % alignment with respect to applied central guide column voltage. Optimal guide voltages are the voltages correlated to the maximum % alignment on each plot. At voltages beyond those indicated by an X the deposition rate was sufficiently slow to inhibit collection.

3.2 Effects of Guide Column Voltage

The degree of fiber alignment was observed to be a function of the magnitude of the voltage applied to the central guide column. Figure 5 and Figure S2 show this relationship between increasing central guide column voltage and increasing degree of alignment for CoFe_2O_4 . As the voltage applied to the central guide column increases, so to does the measured degree of alignment until a maximum alignment is reached. This progression in the degree of alignment demonstrates that the applied guide voltage does indeed affect fiber alignment, and further confirms that any observed alignment is not solely due to the insulating air gap separating the array columns. Increasing the applied central guide column voltage beyond this threshold caused severely reduced deposition in the gaps adjacent to the central column and a deterioration of alignment.

To demonstrate the efficacy of this approach the guide column array was used to electrospin aligned arrays of other ceramic fiber systems, including BaTiO_3 , BiFeO_3 , $\text{Ni}_{0.5}\text{Zn}_{0.5}\text{Fe}_2\text{O}_4$, and an additional CoFe_2O_4 solution spun from a solution with a higher conductivity. The observed trend of increasing alignment with increasing guide column voltage until an optimum guide voltage and maximum alignment were reached was consistent across each system, however the optimum guide voltage magnitude was not. The variance of

optimal alignment guide voltage was thought to be due to the differences in solution conductivity between the different fiber systems. As the conductivity of the precursor solution increases so too would the bending instabilities that occur during electrospinning, requiring greater electrostatic fields to force fiber alignment during deposition. Therefore, greater guide voltages would be needed to create these larger electrostatic fields. Results for these fiber systems can be found in the supplemental information (Figures S3-S6).

3.3 Effects of Solution Conductivity on Alignment

Table 1 and Figure 6 show that a maximum alignment voltage was determined each fiber system. Spinning at voltages greater than the maximum alignment voltage lead to low fiber accumulation as the Coulombic repulsion between the incoming jet and the similarly charged guide column increased. It was also found that at these higher voltages deposition increased on the outermost grounded columns of

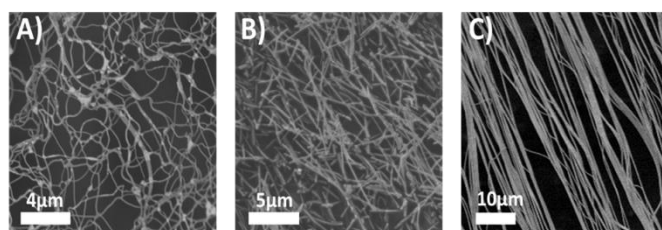


Figure 7. A) Post calcined fibers suspended across platinum boat. B) Post calcined fibers using salt suspension at a ramp rate of 5 °C/min. C) Post calcined fibers using an adjusted, slower ramp rate of 2 °C/min as opposed to the original 5 °C/min used after reaching the polymer burn off temperature.

the array in a predominantly random manner. The most noticeable trend is the relationship between solution conductivity and optimum guide voltage, whereas the conductivity of the solution increases so does the guide column voltage required for obtaining aligned fibers. To exemplify the importance of this relationship in the guide column array, consider two cases: first, two solutions where the ceramic content was identical, but the conductivities were different. Second, two solutions where the ceramic content is different, but the solution conductivities are the same. In the first case, the only difference between the two solutions are their conductivities. To perform this experiment two solutions were prepared using the same composition and concentration of ceramic precursors but aged for different times resulting in conductivities of 1.8 mS/cm for CoFe₂O₄ (1) (Figure 6C) and 3.6 mS/cm for CoFe₂O₄ (2) (Figure 6E). Despite having the same initial ceramic ion content, the differences in solution conductivity caused a difference of 3 kV in optimum guide voltage. For the second case, two solutions of approximately the same conductivity but differing composition were electrospun. Here, CoFe₂O₄ (1) with a conductivity of 1.8 mS/cm (Figure 6C) and BiFeO₃ (Figure 6B) with a conductivity of 1.7 mS/cm were selected. For these two solutions, the optimum guide voltages were both 6 kV, attributed to their nearly identical solution conductivities. This confirms that the alignment guide voltage can be determined using the solution conductivity and that this alignment

technique is suitable for a wide range of phase ceramic systems.

3.4 Calcination

Once aligned mats of as-spun fibers were obtained an additional consideration arose due to the dual ceramic/polymer composition of the fibers. Specifically, the alignment of the mats needed to be maintained while the polymer binder was burned off and the ceramic phase(s) developed without shrinking or sintering together. To ensure the fibers maintained alignment during calcination all the fibers from the array, including the randomly dispersed flanking fibers, were removed and calcined as a single sheet. The randomly dispersed mat overlaid the edges of the aligned fibers, anchoring them in place during calcination. To ensure the polymer removal and ceramic development occurred at appropriate rates the step size of the temperature ramp rate

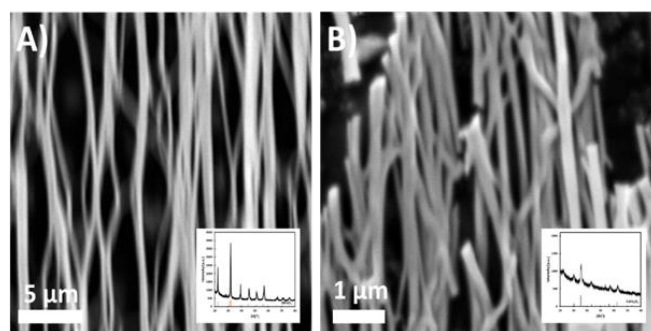


Figure 8. A) Calcined BiFeO₃ with XRD spectra showing hexagonal BiFeO₃. B) Calcined CoFe₂O₄ with XRD spectra showing cubic CoFe₂O₄. XRD spectra are also shown in Figures S6-S7.

during the calcination regimes were reduced compared to

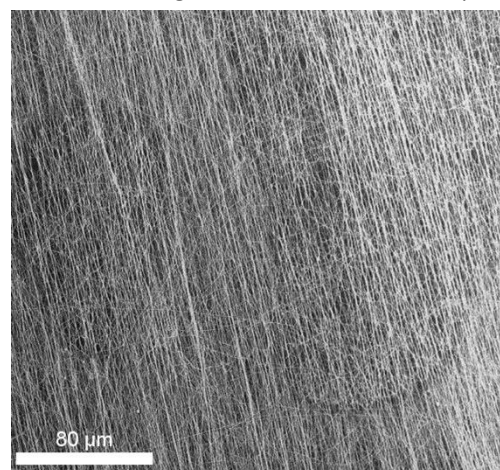


Figure 9. CoFe₂O₄ (1) aligned across two contacts spaced 2 cm apart with an applied voltage of 6 kV to one contact while the other remain grounded.

those for a randomly aligned array.

To optimize the calcination process for maintaining alignment, it was thought that anchoring a fiber mat across an air gap would prevent entanglement and fracture as the ceramic phase developed. Fiber mats were anchored across a

platinum boat and calcined (**Figure 7a**). However, fiber mats did not maintain alignment using this method. It is likely that the shrinkage that occurred during the polymer binder burnout phase resulted in the fibers being unable to span the air gap and collapsing, and losing alignment. A salt calcination method (**Figure 7b**) was then employed to maintain alignment involved, where finely ground sodium chloride acts as a physical barrier between fibers while also providing support to prevent collapse. The success of this method was limited by the extreme difficulty of maintaining alignment while removing the salt from the fiber arrays post calcination. Lastly,

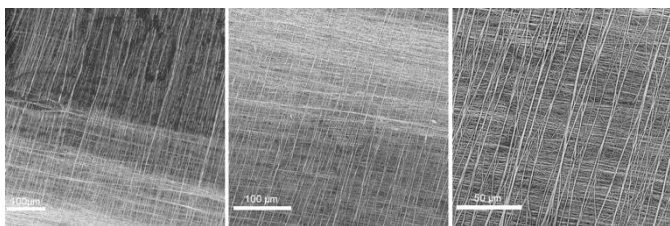


Figure 10. SEM images showing orthogonally patterned CoFe_2O_4 fibers electrospun onto the grid array.

it was theorized that a slower calcining ramp rate could aid in maintaining alignment (**Figure 7c**). The ramp rate after the polymer binder burn off phase at 250°C was reduced from $5^\circ\text{C}/\text{min}$ to $2^\circ\text{C}/\text{min}$. Figures 7b-c show that reducing the ramp rate significantly reduced the loss of alignment during the calcination phase. To verify this calcination regime maintained proper development of ceramic phases as well as maintained alignment, samples of BiFeO_3 and CoFe_2O_4 were calcined with the slower ramp rate regime. Both systems maintained a high degree of alignment as seen in **Figure 8**. In conjunction with maintained alignment, XRD of both samples still produced the desired ceramic phase as shown in the insets of **Figure 8** as well as in **Figures S7-S8**.

To ensure that the slower ramp rate calcination matched the versatility of the guided column array, samples of 70 wt.% BiFeO_3 / 30 wt.% CoFe_2O_4 Janus fibers were also calcined. There was little observed loss of alignment and the Janus bi-phasic morphology was maintained throughout calcination.

3.5 Grid Array

To demonstrate the efficacy of using a guiding voltage a grid array was developed to extend this approach to fabricate more complex arrays of ceramic nanofibers. These more complex assemblies of patterned arrays of ceramic fibers could offer higher control and ordering of properties. To accomplish this, a substrate was designed such that alignment could be obtained in orthogonal directions via two perpendicular pairs of copper plates spaced 2 cm apart as shown in **Figure 2**.

Initial testing was performed by separating two standalone copper plates 2 cm apart via an insulating air gap. CoFe_2O_4 was spun across the gap to simulate the designed substrate and test if alignment could be achieved by applying an electric field between two copper plates. By applying 6 kV to one contact and grounding the opposite contact, alignment was achieved (**Figure 9**).

The success of this initial test led to the construction of the grid array (**Figure 2**), where it was hypothesized that by only electrically contacting two of the four plates during electrospinning would direct aligned deposition between the contacted plates. Thus, one could apply a voltage to a plate and ground the opposite plate as a pair, deposit aligned fibers, disconnect from the pair of plates, connect the orthogonal pair of plates in an identical fashion, and subsequently deposit fibers aligned orthogonally to the originally deposited layer, creating a grid.

Initial trials were conducted using the same conditions, i.e., collector distance and applied voltage, as used for the guide column array, with minimal success. It was thought that since the target area for deposition was significantly reduced (the entire length of a 20 cm column versus a 2 cm diameter circle) that decreasing the spinning distance of needle tip to collection array from 28 cm to 16 cm would result in increased alignment. This decrease in the collector distance conditions yielded fibers in a grid array as shown in **Figure 10**.

The results of initial grid array testing show promise as a technique to generate more complex fiber patterns and arrays. It should be noted that the recorded optimum pattern voltage for the grid array was 2 kV lower than the optimum guide voltage observed for the same precursor solution. This is attributed to the fact that in the grid array the insulating gap is composed of epoxy, which has a higher dielectric constant than air. As a result, as fibers deposit onto the grid array, dipoles are induced on the surface of the epoxy due to interactions with the charged fibers. The higher dielectric constant of the epoxy also decreases the dissipation of charge from the fiber into the insulating gap medium causing the deposited fibers to contribute more to the electrostatic repulsion of the incoming fiber jet. This increases the stability of the alignment achieved by anchoring the fiber on a solid surface as well as reducing the discharge rate of deposited fibers. As a result, lower electric fields are required to maintain alignment, thus reducing the optimum pattern voltage.

To demonstrate the versatility and functionality of the grid array, BaTiO_3 was also electrospun onto the grid array to manufacture a removable mat of patterned fibers for

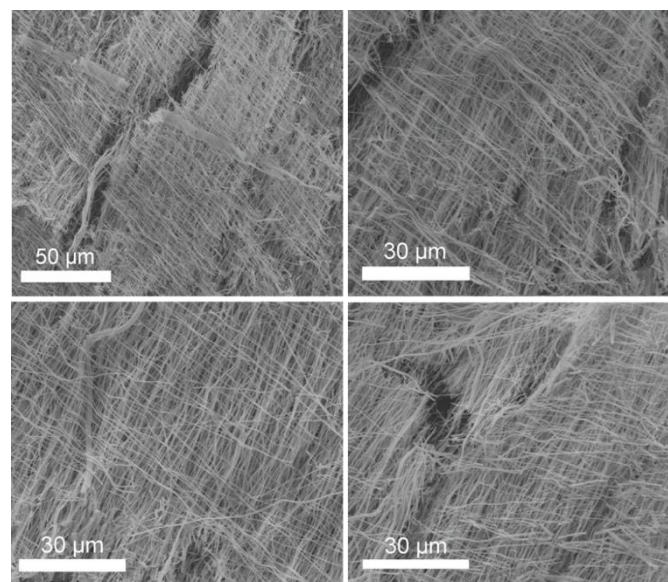


Figure 11. SEM images of patterned, calcined BaTiO_3 fibers. Two discernable, orthogonal layers of aligned fibers are present.

calcination. The patterned fibers were then transferred to a calcination dish. Calcination of the fibers was conducted with the optimized reduced ramp rate regime discussed in Section 3.5 to help maintain fiber orientation as shown in **Figure 11**.

The images in Figure 11 show the presence of two orthogonal layers of calcined fibers. These images demonstrate that the grid array in combination with an optimized calcination regime can produce patterned, calcined arrays of fibers for use in a wide range of applications.

Conclusions

The guide column array presented in this paper has successfully overcome the challenges of electrospinning aligned ceramic fibers. Through the application of a guide voltage in an array of grounded columns the ceramic fibers were electrospun in an aligned configuration utilizing only electrostatic field interactions. These field interactions could be tailored to each fiber system by increasing or decreasing the applied guide voltage depending on the conductivity of the precursor solutions. Thus, no modification of the precursor solutions were necessary. This was successfully demonstrated with five single phase fiber systems, where the morphology of the composite was maintained during the alignment process.

A relationship was built between the precursor solution conductivity and the magnitude of the voltage applied to the array required for maximum alignment so that the voltage applied to the array can be adjusted to match the conductivity of the solution that is desired to be aligned. Though the focus of this manuscript is on ceramic fibers, this method can also be extended to polymer electrospinning solutions once the solution conductivity is known. Further, by making simple alterations to the calcination regimes, the ceramic fibers maintained their alignment through polymer burn out and ceramic calcination. The guide column array is a simple method of aligning already established ceramic electrospinning solutions that could be easily implemented for additional ceramic nanofiber systems to increase the utility of the electrospun fibers. The principles developed for the guide column array were extended to develop an array capable of patterning fibers in a grid.

Conflicts of interest

There are no conflicts to declare.

Acknowledgements

This work was supported by the National Science Foundation through CMMI-1436623. The Research Service Centers of the Herbert Wertheim College of Engineering at the University of Florida are acknowledged for the use of the FEI XL-40 scanning electron microscope, and Panalytical X'PERT powder diffractometer.

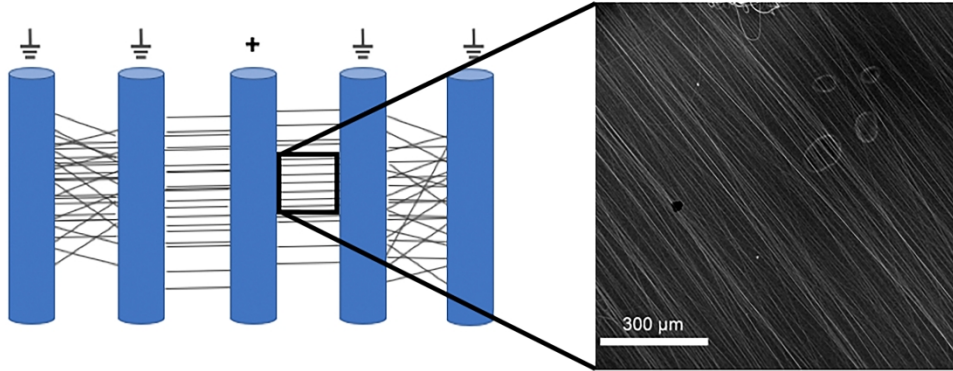
Notes and references

- 1 M. C. Beilke, J. W. Zewe, J. E. Clark and S. V. Olesik, *Anal. Chim. Acta*, 2013, **761**, 201–208.
- 2 E. C. Spivey, Z. Z. Khaing, J. B. Shear and C. E. Schmidt, *Biomaterials*, 2012, **33**, 4264–4276.
- 3 T. Chen, S. Wang, Z. Yang, Q. Feng, X. Sun, L. Li, Z. S. Wang and H. Peng, *Angew. Chemie - Int. Ed.*, 2011, **50**, 1815–1819.
- 4 M. Afshari, *Electrospun Nanofibers*, Deans, Mathew, Cambridge, 2017.
- 5 M. Ma, M. Gupta, Z. Li, L. Zhai, K. K. Gleason, R. E. Cohen, M. F. Rubner and G. C. Rutledge, *Adv. Mater.*, 2007, **19**, 255–259.
- 6 Y. Zhang, X. He, J. Li, Z. Miao and F. Huang, *Sensors Actuators, B Chem.*, 2008, **132**, 67–73.
- 7 W. Sigmund, J. Yuh, H. Park, V. Maneeratana, G. Pyrgiotakis, A. Daga, J. Taylor and J. C. Nino, *J. Am. Ceram. Soc.*, 2006, **89**, 395–407.
- 8 D. Li, J. T. McCann, Y. Xia and M. Marquez, *J. Am. Ceram. Soc.*, 2006, **89**, 1861–1869.
- 9 A. Bajji, Y. W. Mai, Q. Li, S. C. Wong, Y. Liu and Q. W. Yao, *Nanotechnology*, , DOI:10.1088/0957-4484/22/23/235702.
- 10 D. Li, T. Herricks and Y. Xia, *Appl. Phys. Lett.*, 2003, **83**, 4586–4588.
- 11 Dan Li, A. Yuliang Wang, Y. Xia*, D. Li, Y. Wang and Y. Xia, *Nano Lett.*, 2003, **3**, 1167–1171.
- 12 J. D. Starr and J. S. Andrew, *Chem. Commun.*, 2013, **49**, 4151–4153.
- 13 S. H. Xie, J. Y. Li, Y. Qiao, Y. Y. Liu, L. N. Lan, Y. C. Zhou and S. T. Tan, *Appl. Phys. Lett.*, 2008, **92**, 90–93.
- 14 M. Sangmanee and S. Maensiri, *Appl. Phys. A Mater. Sci. Process.*, 2009, **97**, 167–177.
- 15 J. Yuh, J. C. Nino and W. M. Sigmund, *Mater. Lett.*, 2005, **59**, 3645–3647.
- 16 G. C. Gazquez, S. Lei, A. George, H. Gullapalli, B. A. Boukamp, P. M. Ajayan and J. E. Elshof, *ACS Appl. Mater. Inter.*, 8, 2016, 13466–134611.
- 17 M. J. Bauer, C. S. Snyder, C. C. Bowland, A. M. Uhl, M. A. K. Budi, M. Villancio-Wolter, H. A. Sodano and J. S. Andrew, *J. Am. Ceram. Soc.*, 2016, **99**, 3902–3908.
- 18 B. Y. Sir and G. Taylor, .
- 19 D. H. Reneker and A. L. Yarin, *Polymer (Guildf)*, 2008, **49**, 2387–2425.
- 20 D. Li, Y. Wang and Y. Xia, *Adv. Mater.*, 2004, **16**, 361–366.
- 21 Y. Xin, Z. Huang, J. Chen, C. Wang, Y. Tong and S. Liu, *Mater. Lett.*, 2008, **62**, 991–993.
- 22 A. Theron, E. Zussman and A. L. Yarin, *Nanotechnology*, 2001, **12**, 384–390.
- 23 V. P. Secasanu, C. K. Giardina and Y. Wang, *Biotechnol. Prog.*, 2009, **25**, 1169–1175.
- 24 W. E. Teo and S. Ramakrishna, *Nanotechnology*, 2005, **16**, 1878–1884.
- 25 J. . Deitzel, J. Kleinmeyer, D. Harris and N. . Beck Tan, *Polymer (Guildf)*, 2001, **42**, 261–272.
- 26 J. J. Stankus, J. Guan and W. R. Wagner, *J. Biomed. Mater.*

Journal Name

ARTICLE

- Res.*, 2004, **70A**, 603–614.
- 27 L. Buttafoco, N. G. Kolkman, P. Engbers-Buijtenhuijs, A. A. Poot, P. J. Dijkstra, I. Vermes and J. Feijen, *Biomaterials*, 2006, **27**, 724–734.
- 28 G. H. Kim, *J. Polym. Sci. Part B Polym. Phys.*, 2006, **44**, 1426–1433.



298x142mm (300 x 300 DPI)